2020 IEEE International Conference on Robotics and Automation (ICRA)
31 May - 31 August, 2020. Paris, France

Slip-Limiting Controller for Redundant Line-Suspended Robots: Application to LineRanger

Philippe Hamelin*, Pierre-Luc Richard, Marco Lepage, Marin Lagacé,
Alex Sartor, Ghislain Lambert, Camille Hébert and Nicolas Pouliot

Maintenance and Inspection Robotics Department
Hydro-Québec's Research Institute (IREQ)
Varennes, QC, CANADA, J3X 1S1

***Abstract*— In this paper, a slip-limiting controller for redundant line-suspended robots is presented. This kind of robot is usually equipped with v-shaped wheels, which brings uncertainty about the effective wheel radius, particularly when crossing obstacles. The proposed algorithm is able to estimate and limit wheel slippage in the presence of such uncertainty, relying only on wheel angular velocity measurements. Slip limitation occurs in the control allocation algorithm and hence is decoupled from the high-level velocity controller, allowing a broad applicability in centralized control approaches. Experimental results on LineRanger show that it effectively reduces wheel slippage compared to traditional centralized control while being more energy efficient than traditional decentralized control approaches.**

I. INTRODUCTION

Like many electrical utilities around the world, Hydro-Québec operates tens of thousands of kilometers of power transmission lines. The rigorous management of these assets is therefore an important challenge for ensuring reliability and sustainability. One of the maintenance activities is to perform visual inspections for early detection of potential defects. Although drones have become powerful inspection tools [1][2], line-suspended robots remain an effective way to perform several kilometers of inspection per day [3]-[7], offering a close and stable point of view while being less affected by meteorological conditions.

The control of line-suspended robots is a subject that is still underdeveloped compared to other types of mobile robots. Nevertheless, two main control approaches can be discerned: decentralized and centralized.

In decentralized approaches [8], the robot's global setpoint is transformed into individual position or velocity setpoints for each of the wheels based on kinematic equations. Position or velocity control is thus performed by individual control loops at each of the wheels. This approach fits well with distributed electronic architectures where communication between the main processor and the motor drives is limited. Indeed, since the control loop is closed in each of the drives, communication has less influence on the position or velocity tracking performance. However, if there is a kinematic error, such as an unknown variation in the wheels radii, it is impossible to obtain a null tracking error for all wheels due to kinematic constraints, leading to the wheels working against each other. This significantly reduces the efficiency, a major drawback for line-suspended robots, which are typically battery powered.

Figure 1. LineRanger inspecting a 735kV power transmission line

The kinematic error is a common problem as line-suspended robots often have v-shaped wheels, which systematically cause a change in the effective radius of the wheel when crossing an obstacle. Moreover, some line-suspended robots, such as LineRanger [4] (see Figure 1), have non-vertical wheels, which are not naturally self-centering on the conductors. Although the robot is mechanically optimized to target self-centering behavior of its wheels, in real situations this is not always the case. Indeed, misalignment of conductors, very high slopes, twisted wires and mechanical imprecision may lead to variable effective wheel radius. Figure 2 illustrates some possible configurations that lead to different effective radii.

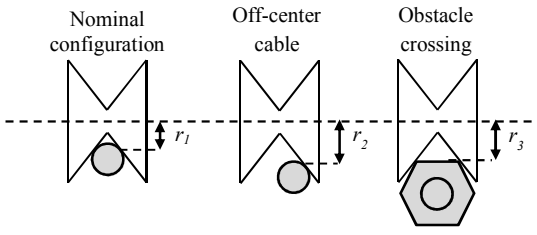

Figure 2. Examples of possible v-shaped wheel configurations on a given conductor with different effective radii.

* Philippe Hamelin can be reached as corresponding author at 450-652-8499 x2198 or at hamelin.philippe@ireq.ca.

In the centralized approach [9] a high-level controller computes a virtual control effort which is then translated into actuator commands using a control allocation algorithm [10]. Hence, instead of controlling the position or velocity of the individual wheels, the global coordinates of the robot are controlled. This approach avoids having several control loops that can potentially work against each other, which is therefore more energy efficient. However, since there is no individual control of the wheels, significant slipping may occur on a wheel if there is a loss of traction, which can occur, for example, while crossing an obstacle or if there is grease on the conductor. This slippage can be detrimental not only to energetic efficiency, but can also affect the stability of the system. It is therefore desirable to apply the centralized approach together with a slip limiting system.

Many studies have been done to control or reduce wheel slipping on wheeled mobile robots [11]-[13]. A wheel slip controller based on fuzzy logic has also been applied recently to a line-suspended robot [14]. Most of these methods require a good knowledge of the wheel radius, which is generally not the case for line-suspended robots given the reasons mentioned above. Some alternative approaches are to use a model-based observer [15] or an external sensor [16] to estimate slippage.

In this paper, we propose a new slip-limiting controller which only relies on the measured angular velocity of the wheels, hence does not require a complex model-based observer nor external sensors. Although also applicable to position control, in this case the method is applied to velocity control. Slippage of each wheel is estimated by taking into account the uncertainty of the effective radius of the wheels. Then, a control allocation problem is formulated such that the torque of the wheel is reduced in proportion to the estimated slip. The proposed method is experimentally validated on LineRanger and the benefits in terms of slip reduction and energy efficiency is demonstrated.

II. Modeling of the Line-Suspended Robot

The aim of this paper is to present a slip-limiting controller, which implies indeed that there is slippage at the wheels. However, a robot dynamic model taking into account slippage via a tire-conductor interaction model is fortunately not required. For the proposed controller design approach, only a pure rolling model is needed.

There are many different line-suspended robot configurations, some of which may include complex mechanisms. The most common configuration has several wheels rolling on the same conductor, or parallel conductors, each producing a force in the same direction [4]-[7]. Under rolling conditions they can be considered redundant single-degree-of-freedom robots, which is the basis for the proposed model. Also, without loss of generality, we assume that each wheel is motorized and has the same properties, i.e. radius, inertia and friction. Using the Lagrangian approach, the following dynamic model is obtained:

$$\left(m+n\frac{I_w}{r^2}\right)\dot{v}+n\frac{b}{r^2}v=\frac{1}{r}\sum_{i=1}^{n}\tau_i+mg\sin(\theta) \qquad (1)$$

where m is the mass of the robot, n is the total number of wheels, I_w is the wheel inertia, r is the nominal wheel radius, g is the gravitational acceleration, θ is the slope of the robot on the catenary, τ_i is the torque applied at the i^{th} wheel, b is the wheel angular viscous friction coefficient and v is the linear velocity of the robot.

To design the nominal velocity controller, it is convenient to use a single-input/single-output (SISO) linear model, whose virtual control effort input is the total linear force produced by the motors and the output is the velocity of the robot. If we consider the gravity force a slowly varying external disturbance that can be neglected, we obtain the following model:

$$\bar{m}\dot{v}+\bar{b}v=u \qquad (2)$$

This equation represents a single-degree-of-freedom mass-damper linear model with $\bar{m}=m+nI_w/r^2$ as the equivalent mass and $\bar{b}=nb/r^2$ as the equivalent damping coefficient. The virtual input u represents the total linear force produced by the motors and is defined by the following linear mapping:

$$u=\mathrm{B}\tau \qquad (3)$$

where $\mathrm{B}\in\mathbb{R}^{1\times n}=\begin{pmatrix}1/r & \cdots & 1/r\end{pmatrix}$ is the control matrix and $\tau\in\mathbb{R}^{n\times 1}=\begin{pmatrix}\tau_1 & \cdots & \tau_n\end{pmatrix}$ is the wheel torque vector. Applying the Laplace transform to (2) leads to the transfer function from the linear force input *U(s)* to the robot velocity *V(s)*:

$$G_p(s)=\frac{V(s)}{U(s)}=\frac{1}{\bar{m}s+\bar{b}} \qquad (4)$$

III. Slip-Limiting Controller

As illustrated in Figure 3, the slip-limiting controller proposed in this paper is divided into three components: the velocity controller, the velocity and slip ratio estimator and the slip-limiting control allocation. The respective roles of each of these components are described in subsequent sections.

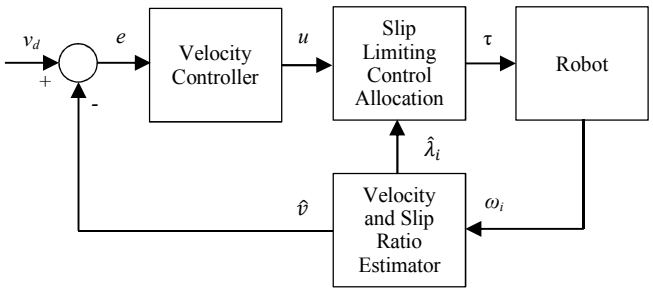

Figure 3. Slip-limiting controller block diagram

A. Velocity controller

As the name suggests, the role of this component is to ensure control of the velocity of the robot. One of the advantages of the proposed method is that the slip limitation is performed by the control allocation algorithm, thus leaving a freedom in the choice of the high-level controller. In this

case, a Proportional-Integral (PI) controller in the Laplace domain is chosen:

$$G_c(s) = \frac{U(s)}{E(s)} = k_p + \frac{k_i}{s} \quad (5)$$

The input is the velocity error and is defined as $e = v_d - \hat{v}$, where v_d is the desired velocity and $\hat{v}$ is the robot estimated velocity provided by the velocity and slip ratio estimator described later. The output is the linear force command *u*. One systematic way to design the PI controller is by using a pole placement method in the Laplace domain. This, however, requires knowledge of the transfer function of the controlled system, which takes place between the command input *u* and the estimated velocity $\hat{v}$. Based on the following two assumptions:

- The slip-limiting control allocation ensures the conservation of the control effort as defined by the linear mapping of eq. (3);
- The velocity and slip ratio estimator provides an accurate estimate of the velocity such that we can consider $\hat{v} \cong v$;

the transfer function (4) can represent the model of the system to be controlled. The closed-loop transfer function is computed as follows:

$$G_{cl}(s) = \frac{G_c(s)G_p(s)}{G_c(s)G_p(s)+1} \quad (6)$$

where $G_p(s)$ and $G_c(s)$ are defined by eqs. (4) and (5) respectively. Then, the second-order characteristic equation $\Delta_d(s) = s^2 + 2\xi\omega_n s + \omega_n^2$ is applied to eq. (6) and solved to obtain the following algebraic solution for the gains:

$$k_p = 2\xi\omega_n\bar{m} - \bar{b} \quad (7)$$

$$k_i = \bar{m}\omega_n^2 \quad (8)$$

where the damping ratio ξ and natural frequency ω_n can be chosen to achieve a desired transient response.

B. Velocity and slip ratio estimator

In order to provide a proper slip-limiting controller, slippage of each wheel must be quantified. A well-known quantity that describes the slip behavior of a wheel is called the slip ratio and is defined as [13]:

$$\lambda = \frac{r\omega - v}{\max(r\omega, v)} \quad (9)$$

where *r* is the wheel radius, ω is the angular velocity of the wheel and *v* is the velocity of the robot. The calculation of the slip ratio raises two issues related to line-suspended robots. First, these robots do not generally have slip-free undriven wheels which would allow an accurate measurement of the velocity *v*. The robot velocity must hence be measured using an external sensor (e.g. inertial navigation system), or, more cost-efficiently, estimated using driven wheel angular velocities. Second, as discussed previously, it is common for line-suspended robots to be equipped with v-shaped wheels, which brings uncertainty to the effective radius *r* of the wheel during obstacle crossing. These two issues must be addressed by the velocity and slip ratio estimator, whose objective is twofold:

- Provide an estimate of the robot velocity $\hat{v}$, which is required by the slip ratio estimation algorithm and the velocity controller;
- Provide an estimate of the slip ratio $\hat{\lambda}_i$ of each *i* wheel, which is required by the slip-limiting control allocation.

The proposed estimation algorithm is an extension of Yuan Ping Li et al. [11], now considering the uncertainty of the wheel radius.

1) Velocity estimation algorithm

To avoid dependence on an external velocity sensor, the proposed velocity estimation algorithm is based purely on the measured angular velocity of each wheel. As commonly stated in the literature [11], it assumes that over *n* wheels, there are $k \in [1, n-1]$ non-slipping wheels, where *k* is a design parameter. Moreover, we assume there is no skidding during braking, since line-suspended robots are mostly subject to slipping when accelerating over obstacles. These two assumptions make it possible to use the following three-step algorithm to estimate robot velocity:

1) Among all *n* wheels, find the *k* non-slipping wheels, i.e. with the smallest absolute angular velocity;
2) Calculate the reference wheel angular velocity $\hat{\omega}$ by taking the average of the *k* non-slipping wheels angular velocities;
3) Calculate the estimated robot velocity from the reference angular velocity, $\hat{v} = r\hat{\omega}$.

2) Slip ratio estimation algorithm

Once an estimate of the robot velocity is obtained by the algorithm of section III.B.1, the slip ratio of each wheel should be calculated according to eq. (9). However, this definition assumes that the radius *r* of the wheel is perfectly known, which is not the case for line-suspended robots equipped with v-shaped wheels, especially when crossing obstacles.

Considering that for a given wheel, the effective radius is within some range, that is $r \in [r_{\min}, r_{\max}]$, then, a worst-case scenario would be that one wheel has an effective radius of $r_{\min}$ while for another it is $r_{\max}$. In this case, even if there is no slippage, there would be a factor of $r_{\max} / r_{\min}$ between their measured angular velocities. The algorithm must therefore consider this uncertainty on the effective radius *r* to avoid declaring a wheel slip when there is none. In addition, it is impossible to measure the slip of a wheel whose velocity factor is less than or equal to $r_{\max} / r_{\min}$, since this case is kinematically indistinguishable from that described above. Assuming as in section III.B.1 there is no skidding, the slip-ratio of the i^{th} wheel can be estimated as follows:

$$\lambda_i = \begin{cases} \dfrac{|\omega_i| - \max\left(\dfrac{r_{\max}}{r_{\min}}|\hat{\omega}|, \varepsilon\right)}{|\omega_i|} & \text{if } |\omega_i| > \max\left(\dfrac{r_{\max}}{r_{\min}}|\hat{\omega}|, \varepsilon\right) \\ 0 & \text{otherwise} \end{cases} \quad (10)$$

where ω_i is the measured angular velocity of the i^{th} wheel, $\hat{\omega}$ is the reference wheel angular velocity computed by the velocity estimation algorithm of section III.B.1 and ε is a positive scalar determined empirically to account for gear backlash and sensor noise particularly present at low speed. Note that the slip ratio estimation of eq. (10) is bounded, that is $\lambda_i \in [0,1]$.

C. Slip-limiting control allocation

The concept of control allocation is to coordinate the control effort of individual actuators based on a virtual control effort provided by a high-level motion algorithm [10]. This is particularly relevant for over-actuated systems, such as the redundant line-suspended robots considered in this paper. In this case, the control allocation problem means defining a mapping between the virtual control effort calculated by the velocity controller, that is the linear force u to the wheel torque vector τ. Moreover, with respect to the linearized dynamic model expressed by eq. (2), this mapping must guarantee conservation of the control effort such that eq. (3) still stands. Hence, it is equivalent to solving the inverse of eq. (3), for which there is no unique solution.

For unconstrained linear control allocation problems, common practice is to use the weighted generalized inverse of the control matrix B to obtain a solution for u [10], that is:

$$u = \mathrm{W}^{-1}\mathrm{B}^{\mathrm{T}}\left(\mathrm{B}\mathrm{W}^{-1}\mathrm{B}^{\mathrm{T}}\right)^{-1}\tau \quad (11)$$

where $\mathrm{W} \in \mathbb{R}^{n\times n}$ is a positive definite weighting matrix. As an example, if W is defined as an identity matrix then the control effort will be uniformly applied to each wheel. In order to implement the slip limiting behavior, the weighting matrix W is designed such that the wheel torque is inversely proportional to its slip ratio, that is:

$$\mathrm{W} = diag\left(\gamma_1, \ldots, \gamma_n\right) \quad (12)$$

$$\gamma_i = \begin{cases} \varepsilon_\gamma & \text{if } \lambda_i \geq \lambda_{\max}\left(1-\varepsilon_\gamma\right) \\ \dfrac{\lambda_{\max} - \lambda_i}{\lambda_{\max}} & \text{otherwise} \end{cases} \quad (13)$$

where $0 < \varepsilon_\gamma \ll 1$ is a small scalar value to ensure the positive definiteness of the W matrix and $\lambda_{\max}$ is the slip ratio threshold where the wheel torque should be minimal. As a guideline, a lower value of $\lambda_{\max}$ would lead the algorithm to react more promptly to a wheel slip.

IV. Experimental Validation on LineRanger

A. System description

The proposed slip-limiting controller is experimentally validated on LineRanger [4], a four-wheel drive line-suspended robot designed to roll on bundled high-voltage power lines. This robot is a good candidate as it strongly embodies the problems addressed by the proposed controller, namely:

- Its innovative mechanical concept allows it to cross various obstacles present on high voltage power lines, but in return this leads to a loss of adherence and thus wheel slipping;
- The only measurements available are the driving wheel velocities;
- The v-shaped wheels positioned at an angle on the conductor bring major uncertainty to the effective wheel radius.

The physical parameters of LineRanger used to design the controller are described in Table I.

TABLE I. LineRanger Parameters

Parameter	Symbol	Value
Robot equivalent mass	$\bar{m}$	51.6 kg
Robot equivalent viscous friction	$\bar{b}$	46.4 N·s/m
Nominal wheel radius	r	70 mm
Min. wheel radius	$r_{\min}$	70 mm
Max. wheel radius	$r_{\max}$	115 mm
Number of wheels	n	4

B. Controller design

As described in section III, the slip-limiting controller has three components, each with adjustable parameters summarized in Table II.

The k_p and k_i gains were computed using the pole placement method as defined by eqs. (7) and (8). A damping ratio of $\xi = 1$ and a natural frequency of $\omega_n = 18.98$ rad/s are chosen to obtain a critically damped response and a settling time of 0.25 seconds. The slip ratio velocity estimator tolerance ε and the maximum slip ratio threshold $\lambda_{\max}$ were tuned empirically to obtain a good trade-off between promptness and the noise sensitivity of the slip limitation algorithm.

TABLE II. Slip-Limiting Controller Parameters

Parameter	Symbol	Value
Velocity controller proportional gain	k_p	1911.6
Velocity controller integral gain	k_i	18577.4
Slip ratio estimator velocity tolerance	ε	2.0 rad/s
Maximum slip ratio threshold	$\lambda_{\max}$	0.75
Control allocation weight epsilon	ε_γ	10^{-6}
Number of non-slipping wheels	k	2

C. Experimental results

For experimental validation three different methods for controlling the robot were compared, which are described as follows:

a) *Decentralized PI controller (DPIC)*: The velocity is controlled independently at each wheel, each having its own PI controller.
b) *Non slip-limiting controller (NSLC)*: The velocity is controlled using the proposed centralized approach, but with slip limitation disabled, i.e. the weighting matrix W of eq. (12) is set to identity.
c) *Slip-limiting controller (SLC)*: The velocity is controlled using the proposed centralized approach, including slip limitation.

Analogous to car traction systems, DPIC behaves like a locked differential, NSLC is similar to an open differential and SLC to an open differential with traction control. This comparison evaluates the proposed slip-limiting controller according to two important qualities for line-suspended robots. The first is the ability to reduce slippage when there is a loss of traction, mainly during obstacle crossing which requires much more torque. Also, slipping may generate undesirable robot behavior during this critical phase and should be avoided as much as possible. The second is energetic efficiency, which is critically important for these robots that are typically battery powered. Two different experiments were conducted to validate the proposed slip-limiting controller, each focusing on one of the two qualities.

1) Obstacle crossing experiment

The obstacle crossing experiment consists in executing a short trajectory that includes an obstacle crossing, which in this case is a power line suspension clamp (see Figure 4). The detailed crossing sequence of LineRanger is described in [4]. There are many types of clamps with as many kinds of geometries that affect the wheels differently. In this experiment, a very large clamp with non-flat geometry was chosen as one of the most severe obstacle crossings for LineRanger. The target velocity was set to 0.1 m/s for a total distance of about 1.3 meters.

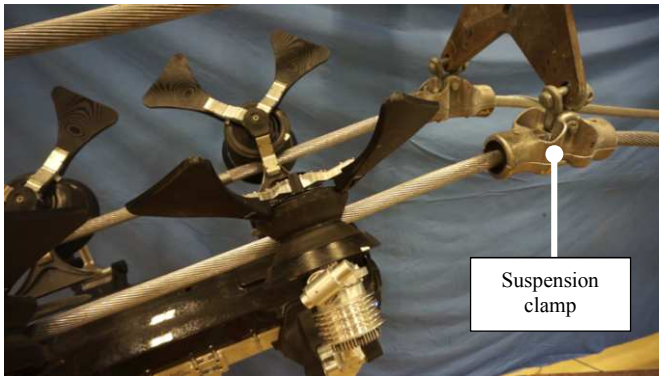

Figure 4. Obstacle crossing experiment

The wheel angular velocities were measured during the experiment. For ease of interpretation, the values have been converted to tangential velocities using the nominal radius of the wheel as shown in Figure 5. For the first quality, slip limitation, DPIC is definitely best. Indeed, by applying the same velocity at each wheel there was essentially no measurable wheel slip. NSLC gave the worst results. With the same torque applied on each wheel, when there is loss of traction on one wheel during obstacle crossing, its velocity increases quickly as the wheel slips. For visualization purposes, the tangential velocity axis of Figure 5 is clipped to 1.0m/s, but in fact we measured peak values up to around 3.0m/s. It is therefore clear that this approach is inadequate without a slip limitation algorithm. Clearly, the results show that by activating the slip limitation in the proposed method (SLC), there is a drastic reduction of wheel slip.

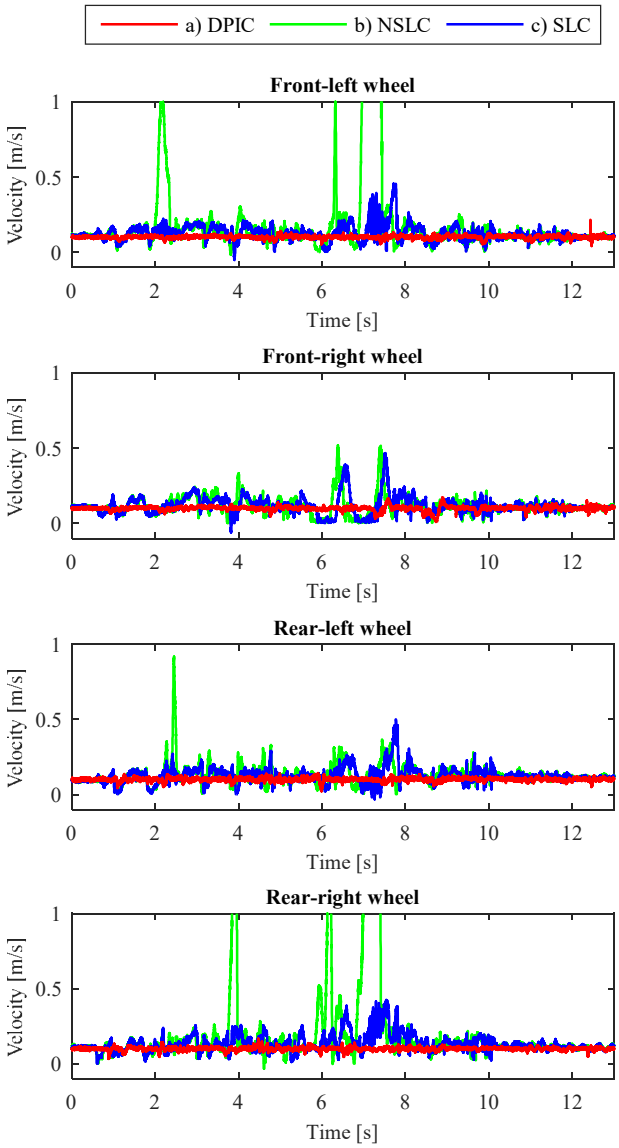

Figure 5. Wheel tangential velocities during obstacle crossing experiment

For the counterpart of DPIC when there is some mismatch between wheels radii, which is almost always the case experimentally, the decentralized PI controllers end up working against each other. This leads to poor energy efficiency, as can be seen in Figure 6 representing the electrical power consumed during the experiment. The power is integrated over time to obtain the total energy consumed, as shown in Table III. Although the short obstacle crossing experiment is not representative enough to allow drawing a final conclusion about energy efficiency, one sees nevertheless, that the proposed SLC method makes it possible to reduce energy consumption by approximately 40% compared to DPIC. With regard to NSLC, the efficiency

is not significantly better than DPIC because of the high electrical power drawn during wheel slipping.

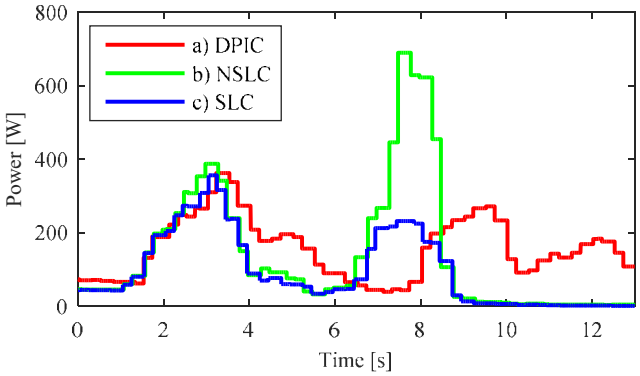

Figure 6. Electrical power consumption during obstacle crossing experiment

TABLE III. ENERGY CONSUMPTION DURING OBSTACLE CROSSING EXPERIMENT

Control method	Energy Consumption [W·h]
a) Decentralized PI controller (DPIC)	0.567
b) Non slip-limiting controller (NSLC)	0.503
c) Slip-limiting controller (SLC)	0.342

2) Long distance round trip experiment

The objective of this experiment was to compare the energy consumption of each of the methods over a representative distance. In this scenario, the robot performed a round trip of about 125m at various velocities on a full-scale power line with a slope ranging from 10 to 15 degrees (see Figure 7). Along this path, there were no obstacles and therefore no wheel slip, which led to equivalent results for NSLC and SLC, so the experimental results were combined.

Figure 7. Long distance round trip experiment on a full-scale power line

Figure 8 illustrates the total energy consumption for all velocities tested. The results clearly illustrate the advantage of the proposed centralized approach (NSLC, SLC) in terms of energy efficiency over the decentralized approach (DPIC), hence giving to LineRanger significantly more autonomy. In addition, from Figure 8 one can deduce that the most efficient traveling velocity was approximately 1 m/s. Figure 9 shows the power consumption versus time for this specific velocity, including both ascent and descent on the line. For NSLC and SLC, it can be seen that, as expected, the slope variation along the trajectory is directly reflected in the power consumption. Regeneration of power was even measured during the descent. This was not noticeable with DPIC, since it was masked by the losses created by the interaction between the PI controllers on each of the wheels. In a typical inspection scenario, the robot spends much more time rolling on the conductor at speeds below 1.0m/s than crossing obstacles. Taking the most conservative case at 1.0m/s, the robot would travel about 62% more distance with SLC compared to DPIC.

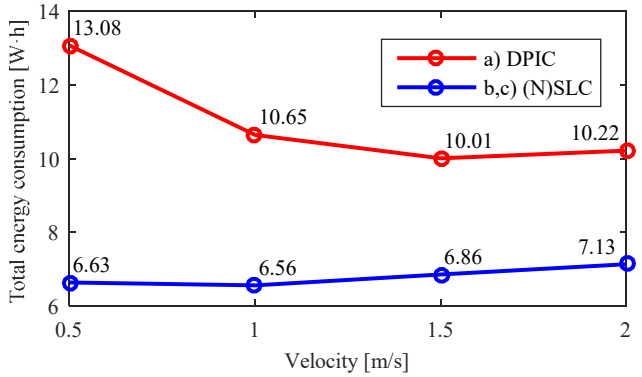

Figure 8. Total energy consumption of long distance round trip experiment for various velocities

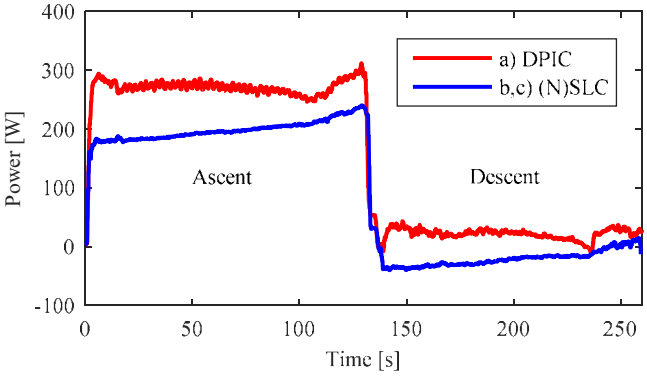

Figure 9. Power versus time of long distance round trip experiment at 1.0 m/s on a full-scale power line

V. CONCLUSION

In this paper, we proposed a new slip-limiting controller for line-suspended robots, which relies only on angular velocity measurements of the wheels. It is able to take into account the uncertainty on wheel radius, which is generally the case for line-suspended robots, typically equipped with v-shaped wheels. The proposed centralized controller (SLC) was successfully validated under real conditions on LineRanger and compared with two other methods: a traditional decentralized approach (DPIC) and the same proposed controller with slip limitation disabled (NSLC). Although DPIC showed less wheel slipping, it is much less energy efficient than SLC or NSLC. In addition, by comparing NSLC to SLC, we showed that the slip limitation algorithm leads to a major reduction in wheel slippage and energy consumption while crossing obstacles, hence demonstrating the benefits of applying slip limitation when using centralized control approaches.

REFERENCES

[1] F. Mirallès et al., "LineDrone Technology: Landing an Unmanned Aerial Vehicle on a Power Line," 2018 IEEE International Conference on Robotics and Automation (ICRA), Brisbane, QLD, 2018, pp. 6545-6552.

[2] A. Varghese, J. Gubbi, H. Sharma and P. Balamuralidhar, "Power infrastructure monitoring and damage detection using drone captured images," 2017 International Joint Conference on Neural Networks (IJCNN), Anchorage, AK, 2017, pp. 1681-1687.

[3] S. Montambault and N. Pouliot, "Hydro-Québec's Power Line Robotics Program: 15 years of development, implementation and partnerships," Proceedings of the 2014 3rd International Conference on Applied Robotics for the Power Industry, Foz do Iguaçu, 2014, pp. 1-6.

[4] P.L. Richard, N. Pouliot, F. Morin, M. Lepage, P. Hamelin, M. Lagacé, A. Sartor, G. Lambert and S. Montambault, "LineRanger: Analysis and Field Testing of an Innovative Robot for Efficient Assessment of Bundled High-Voltage Powerlines", Proceedings of the 2019 International Conference on Robotics and Automation (ICRA), Montreal, 2019.

[5] L. Wang, Fei Liu, Zhen Wang, Shaoqiang Xu, Sheng Cheng and Jianwei Zhang, "Development of a practical power transmission line inspection robot based on a novel line walking mechanism," 2010 IEEE/RSJ International Conference on Intelligent Robots and Systems, Taipei, 2010, pp. 222-227.

[6] P. Debenest et al., "Expliner - Robot for inspection of transmission lines," 2008 IEEE International Conference on Robotics and Automation (ICRA), Pasadena, CA, 2008, pp. 3978-3984.

[7] Yue, Xiang, Hongguang Wang, and Yong Jiang. "A Novel 110 kV Power Line Inspection Robot and Its Climbing Ability Analysis," International Journal of Advanced Robotic Systems, Volume 14, No. 13, May 2017.

[8] Jin Jian, Zhang Guoxian and Zhang Tingyu, "Design of a mobile robot for the innovation in power line inspection and maintenance," 2009 ASME/IFToMM International Conference on Reconfigurable Mechanisms and Robots, London, 2009, pp. 444-449.

[9] Ludan Wang, Sheng Cheng, Jianwei Zhang and Ying Hu, "Control of a redundantly actuated power line inspection robot based on a singular perturbation model," 2008 IEEE International Conference on Robotics and Biomimetics, Bangkok, 2009, pp. 198-203.

[10] Tor A. Johansen, Thor I. Fossen, "Control allocation—A survey," Automatica, Volume 49, No. 5, 2013, pp. 1087-1103.

[11] Yuan Ping Li, M. H. Ang and Wei Lin, "Slip modelling, detection and control for redundantly actuated wheeled mobile robots," 2008 IEEE/ASME International Conference on Advanced Intelligent Mechatronics, Xian, 2008, pp. 967-972.

[12] Y. Tian and N. J. Sarkar, "Control of a Mobile Robot Subject to Wheel Slip," Journal of Intelligent & Robotic Systems, Volume 14, June 2014, pp. 915-929.

[13] T. L. Lam, H. Qian and Y. Xu, "Longitudinal wheel-slip control for four wheel independent steering and drive vehicles," 2014 IEEE International Conference on Robotics and Automation (ICRA), Hong Kong, 2014, pp. 5280-5285.

[14] Y. Yan, X. Liu, H. Guo, J. Li and L. Liu, "Research on Walking Wheel Slippage Control of Live Inspection Robot," 4th International Conference on Mechanics and Mechatronics (ICMMR), Volume 224, Conference 1, 2017.

[15] Hartani, K., Khalfaoui, M., Merah, A., and Aouadj, N., "A Robust Wheel Slip Control Design with Radius Dynamics Observer for EV," SAE Int. J. Veh. Dyn., Stab., and NVH, Volume 2, No. 2, 2018, pp. 135-146.

[16] O.P. Belousova and P.Y. Belousov, "Measurement of the radius and slip velocity of a rolling wheel by a laser Doppler anemometer," Optoelectronics, Instrumentation and Data Processing, Volume 47, No. 2, 2011, pp. 194–202.